Polímeros
ISSN 1678-5169 (Online)

https://doi.org/10.1590/0104-1428.20250053

ORIGINAL ARTICLE

Exploring urea and cross-linkers in alginate films for agricultural seedlings

Nivaldo Ramos Júnior[1], Ana Paula Testa Pezzin[1] and Denise Abatti Kasper Silva[1]*

[1]Laboratório de Materiais, Programa de Pós-graduação em Engenharia de Processos, Universidade da Região de Joinville – UNIVILLE, Joinville, SC, Brasil

**denise.abatti@univille.br*

Abstract

Replacing petroleum-based packaging with biodegradable materials encourages the development of polymers from renewable sources such as sodium alginate, which is biodegradable and abundant in brown algae. The goal of this study was to promote sustainable seedling packaging practices by producing sodium alginate films enriched with urea and glycerol as plasticizers, which were then cross-linked with calcium, fumaric acid, or adipic acid. In this study, both 27 wt% urea and 10 wt% glycerol was used, and the alginate films were prepared by casting with 3 or 10 wt% cross-linker. Thermogravimetric analysis showed that films containing urea exhibited greater thermal stability. FT-IR spectroscopy revealed the formation of partial cross-links between alginate and the cross-linkers, which improved the mechanical and viscoelastic properties. Films cross-linked with calcium ions suggesting that urea does not significantly alter alginate, but contributes to film rigidity, which limits their application for the intended purpose.

Keywords: *biodegradable polymer, sodium alginate, cross-linkers.*

Data Availability: All data supporting the findings of this study are included in this article and its supplementary materials.

How to cite: Ramos Júnior, N., Pezzin A. P. T., & Silva, D. A. K. (2026). Exploring urea and cross-linkers in alginate films for agricultural seedlings. *Polímeros: Ciência e Tecnologia*, *36*(1), e20260011. https://doi.org/10.1590/0104-1428.20250053

1. Introduction

One of the sectors that has increasingly used plastic inputs is agriculture, with an estimated consumption of 12.5 million tons[1]. Among the products that cause soil contamination is the use of plastic bags for growing agricultural seedlings. From this standpoint, substituting this type of packaging for a biodegradable material that ensures seedling transfer may be a plausible alternative.

Alginate, a naturally derived polysaccharide, has garnered significant attention in various fields due to its unique properties and versatile applications, which include 3D bioprinting, drug delivery systems, and sorptive properties[2], producing wound dressings and tissue engineering scaffolds, owing to its biocompatibility, biodegradability, and ability to form hydrogels[3]. The degradation of sodium alginate primarily yields oligosaccharides and monosaccharides, which are non-toxic and can be absorbed by microorganisms without harming the environment. These environmentally friendly features of sodium alginate make it a choice for application in the biomedical, pharmaceutical, cosmetics, textiles, and food science industries[3]. These sustainable characteristics make the alginate biopolymer suitable for environmental remediation, such as the adsorption of dyes and metals[4,5] and the controlled release of fertilizers[6]. When modified[7] or enriched with components such as urea, alginate can improve its mechanical properties and control the release of essential nutrients, such as nitrogen and carbon into the soil[7]. Additionally, the dispersion of nutrients in alginate films can reduce losses from volatilization and leaching[8-11].

On the other hand, researchers have explored the use of carboxylic acids[12-14] for polysaccharide crosslinking; the primary example is citric acid (CA)[15]. Films with this composition are important for exploring the diffusion process, both for delivering substances and for retaining water. The hypothesis was to verify whether alginate films could be partially cross-linked using other organic acids, such as adipic[16,17] and fumaric[8,18] acids. This study seeks to develop urea-enriched alginate films and evaluate the impact of different cross-linking agents on their physical, thermal, mechanical, and biodegradation properties.

2. Materials and Methods

2.1 Materials

Sodium alginate (viscosity: 15-25 cycles per second, 1% in water) and Fumaric acid (99% T) were purchased from Sigma Aldrich Co., Ltd. Adipic acid (99.5% T) was obtained from Êxodo científica, calcium chloride ($CaCl_2$) was supplied by Labsynth Ltd.. Urea was obtained from Tianjin Kaitong Chemical Reagent Co., Ltd. Glycerol was purchased from Sigma Aldridge Co., Ltd.

2.2 Incorporation of urea into alginate

Sodium alginate (6 g) was dissolved in 200 mL type 1 ultrapure water (Milli-Q) containing urea, 27% w/w, and this mixture was heated under reflux at 50 °C for 3 h[5]. The AlgUr sample was collected, frozen, lyophilized, and stored in a desiccator until films were produced.

2.2 Preparation of the films

A mass of 2.5 g of polymer was dissolved in 125 mL of deionized water under moderate magnetic stirring at a temperature of 45 ± 5 °C for 1 h. After complete dissolution, 0.250 g glycerol was added, and the mixture was stirred at 50 °C. The homogeneous solution was divided into two containers (20 × 20 × 5 cm) of 60 mL each and then placed in an oven at 80 °C for 6 h. After drying, the films were stored in a desiccator for 48 h. Two calcium chloride ($CaCl_2$) solutions of 3% and 10% (w/w) in 300 mL of distilled water were prepared for cross-linking. The films were immersed in these solutions for 10 min and then washed with distilled water to prevent the accumulation of crystals on the film surface. The films were then placed in an oven at 30 °C for 6 h and stored in a desiccator for 48 h until further characterization. These films were identified as AlgGlCa 3%, AlgGlCa 10%, AlgUrGlCa 3%, and AlgUrGlCa 10%, respectively.

After complete alginate and glycerol dissolution, the solution was divided into two beakers to prepare solutions containing 3 and 10% fumaric acid (Fu) or adipic acid (Ad). For cross-linking with acids, the procedure followed the protocol described previously[19]. The entire process was performed under stirring at 50 °C. The solutions were poured into the containers and placed in an oven at 80 °C for 8 h to promote cross-linking. Subsequently, the films were removed from the molds and stored for characterization, identified as AlgGlFu 3%, AlgGlFu 10%, AlgUrGlFu 3%, AlgUrGlFu 10% and with as AlgGlAd 3%, AlgGlAd 10%, AlgUrGlAd 3%, AlgUrGlAd 10%).

2.3 Preliminary characterization of alginate films, alginate with urea, and pure components

In this phase, the Fourier Transform Infrared Spectroscopy (FTIR) technique was used to identify the effects of each component on the spectral profile of alginate. Using a Perkin Elmer Frontier equipment with an ATR accessory, 32 scans were performed in the range of 4000 to 650 cm^{-1}, with a resolution of 4 cm^{-1}.

In addition, thermogravimetric analysis (TGA) was performed. The samples were heated from 25 °C to 600 °C at 10 °C/min under an inert atmosphere (N_2) using TGA-Q50 equipment (TA Instruments). TG/DTG curves were obtained using TA Universal Analysis software.

2.4 Characterization of alginate-based and modified alginate-based films

The films produced were characterized by FTIR and TGA under the same conditions described in Section 2.3. DSC was used to characterize the samples. DSC curves were obtained under a dynamic nitrogen atmosphere (50 mL min^{-1}) using hermetically sealed aluminum crucibles containing 4-5 mg of the sample. The temperature range used was 25-400 °C, at a heating rate of 10 °C min^{-1}, using TA Instruments DSC Q20 equipment. The results were analyzed using TA Universal Analysis software, allowing the verification of the effect of polymer modifications on the glass transition temperature (Tg) of the films. Mechanical characterization of the films was performed on a NETZSCH DMA dynamic-mechanical analyzer, model 980, at a frequency of 2.5 Hz in the temperature range of −90 to 130 °C. The test specimens were obtained as films with dimensions of 30 × 5 × 1 mm. Nitrogen gas was used at a heating rate of 2 °C·min^{-1}.

To evaluate the biodegradation of the films, the soil was previously prepared in agreement with ASTM G160-98, then was placed in 1 L beaker cups, approximately 15 cm high, and kept at 30 °C with relative humidity of 85-95%. After, the films were cut to the dimensions 5 cm x 5 cm, dried in an oven with air circulation at 20 °C for 24 h, weighed, inserted into nylon casings with a mesh that allowed exchange with the soil, and then buried in a beaker. This test was performed in duplicate. The effect of the film's degradation was monitored over 42 days. The samples were removed every 7 days, carefully cleaned them with a soft brush and visually inspected.

3. Results and Discussions

3.1 Infrared spectroscopy – FTIR

In the first step, the pure alginate film was characterized to demonstrate the effect of urea and glycerol on the films (Figure 1).

The alginate spectrum was typical, presenting a band between 3600 and 3100 cm^{-1}, characteristic of O-H stretching, bands at 1590 cm^{-1} and 1410 cm^{-1} attributed to the asymmetric and symmetric stretching of the carboxylate group (O-C-O), respectively. Furthermore, in the region between 1330 and 1000 cm^{-1}, shoulders and peaks characteristic of the pyranose group were observed at 1297 cm^{-1}, associated with the angular deformation of C-C-H and O-C-H. The peaks at 1080 and 1020 cm^{-1} were associated with C-O and C-C stretching, respectively. The band at 815 cm^{-1} was related to mannuronic acid residues[20,21]. For urea, two bands (doublets) between 3500 and 3250 cm^{-1} refer to the asymmetric and symmetric N-H stretching of the primary amine, respectively[22]. The band at 1675 cm^{-1} was attributed to carbonyl (C=O) and identified as amide band I, followed by the band at 1600 cm^{-1} attributed to the angular deformation of NH_2, the bands at 1458 cm^{-1} related to the stretching of the C-N bond, and the band at 1150 cm^{-1} attributed to the rocking deformation of primary amines[23,24]. The glycerol spectrum showed a broad absorption band at 3300 cm^{-1}, characteristic of O-H stretching from the alcohol groups. The bands at 2937 and 2878 cm^{-1} were attributed to the stretching mode of the C-H bonds, including a band at 1660 cm^{-1} corresponds to the angular deformation (bending) of the -OH group and one band at 1417 cm^{-1} may be related to the angular deformation of -CH_2. In addition, the 1110 and 1035 cm^{-1} absorptions were attributed to the C-O stretching of secondary and primary alcohols, respectively[25].

The physical characteristics of the films were also distinct, with those of AlgUr being more flexible than Alg. For the control film (Alg10%G), preserved the main band of alginate and glycerol, the band observed at 1040 cm^{-1} can be attributed to C-O stretching groups[26], including the asymmetric and symmetric stretching vibrations of COO^- at wavenumbers of 1598 and 1411 cm^{-1}, respectively[27,28]. The alginate film with urea (AlgUr) is the sum of these two components, while alginate-urea films with glycerol (AlgUr 10%G) show overlap of mainly bands as OH and NH stretching bands around 3300 cm^{-1}, a slight shift to lower wavenumbers for the amide I band at 1654 cm^{-1} and NH_2 stretching observed at 1596 cm^{-1}.

Those generated via ionic cross-linking (Ca^{2+}) are shown in Figure 2.

The alginate-based films (AlgGli) presented the bands predicted and already described for the alginate-glycerol film. A close look at the band corresponding to the stretching of the carboxylate ion (gray line) revealed a slight shift to lower wavenumbers from 1600 cm^{-1} to 1590 cm^{-1}. This change can be associated with the interaction of the regular homopolymer chain with sodium ions and the change in density, radius, and atomic mass when Ca^{2+} replaces Na^+ [29]. Furthermore, there was a decrease in the intensity of the characteristic bands of alginate, such as the -OH stretching band around 3300 cm^{-1} and the asymmetric and symmetric stretching

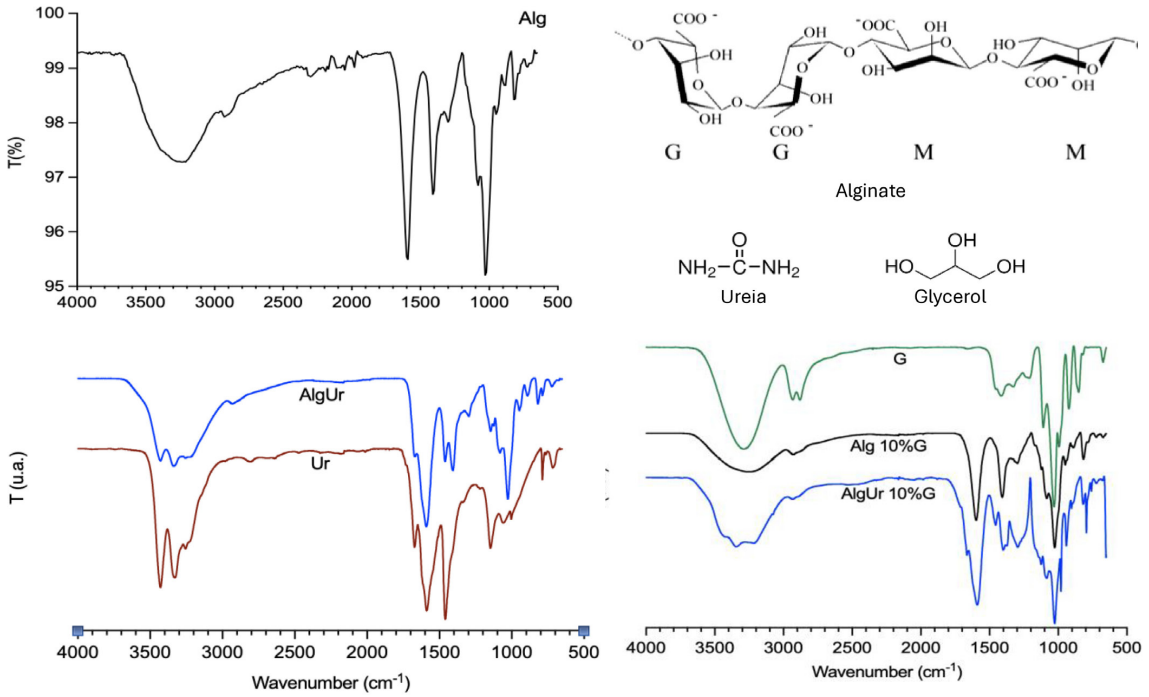

Figure 1. FT-IR spectra of alginate-based films: alginate (Alg), alginate with urea (AlgUr), pure urea (Ur), and glycerol (G), and their respective structural forms. Alginate being composed of blocks of α-L-guluronic acid (G block) and β-D-mannuronic acid (M block).

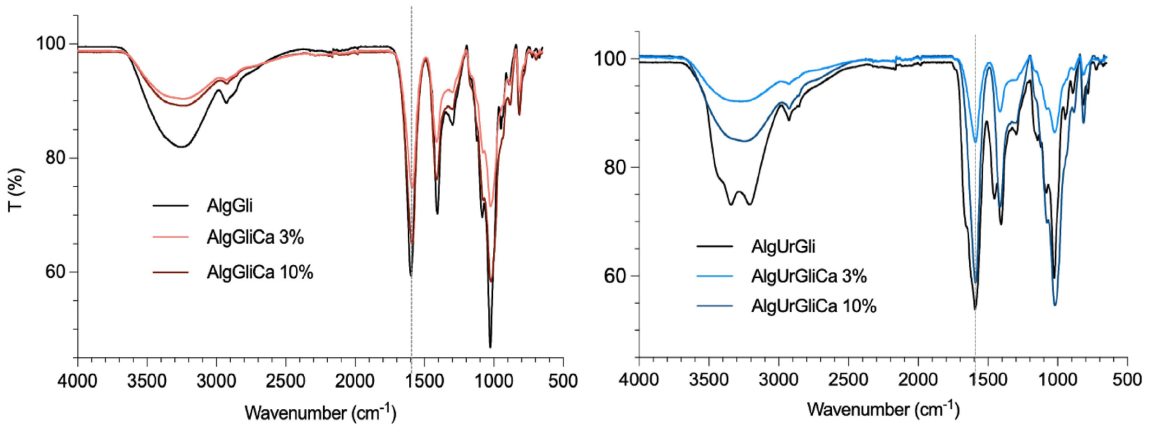

Figure 2. FTIR spectra of alginate-based films (AlgGli) and urea-modified alginate (AlgUrGli) containing 10% glycerol and cross-linked with 3% or 10% (w/w) Ca^{2+} ions.

bands of the carboxylate anion around 1600 and 1400 cm^{-1}, respectively, suggesting that there was an interaction between the hydroxyl and carboxylate groups of alginate and Ca^{2+} ions in the formation of the chelating structure.

The AlgUrGl sample presented overlapping bands for the O-H/N-H and carbonyl groups, as discussed above. However, bands related to the presence of urea were not evident in the samples after being submerged in solutions containing Ca^{2+} ions. Considering the similarities observed between the spectra of the AlgUrGli samples and the AlgGli samples, suggesting that at least part of the urea was removed from the films, which implies a reduction in the nitrogen content of the sample. However, although the shift of the carboxyl band (gray dotted line) was discrete, there was a reduction in the intensity of this band, it was attributed to the hydroxyl group, indicating the interaction of Ca^{2+} ions.

Figure 3 shows a change in the 1750-1730 cm^{-1} region, indicative of cross-linking, in the fumaric and adipic acid samples through the formation of ester bonds. This discrete modification was also observed when carboxymethyl cellulose was cross-linked with citric acid[30]. In the case of the AlgGliFu and AlgGliAd 3% samples, there was also a reduction in the OH bands (3300 cm^{-1}), and that related to the C-OH stretching at 1410 cm^{-1}, which reinforces the hypothesis of partial cross-linking of these films with these acids.

Analogous to the sample without urea, the spectra of AlgGliUr samples with 3 and 10% fumaric and adipic acids were similar. There was also a subtle change in the region 1750-1730 cm^{-1}, indicative of cross-linking through the formation of ester bonds, demonstrating that the acids acted as cross-linkers, at least partially.

3.2 Thermogravimetric analysis – TGA

Figure 4 illustrates the thermal degradation profiles of the films cross-linked with calcium in the absence and presence of urea, and the data are summarized in Table 1.

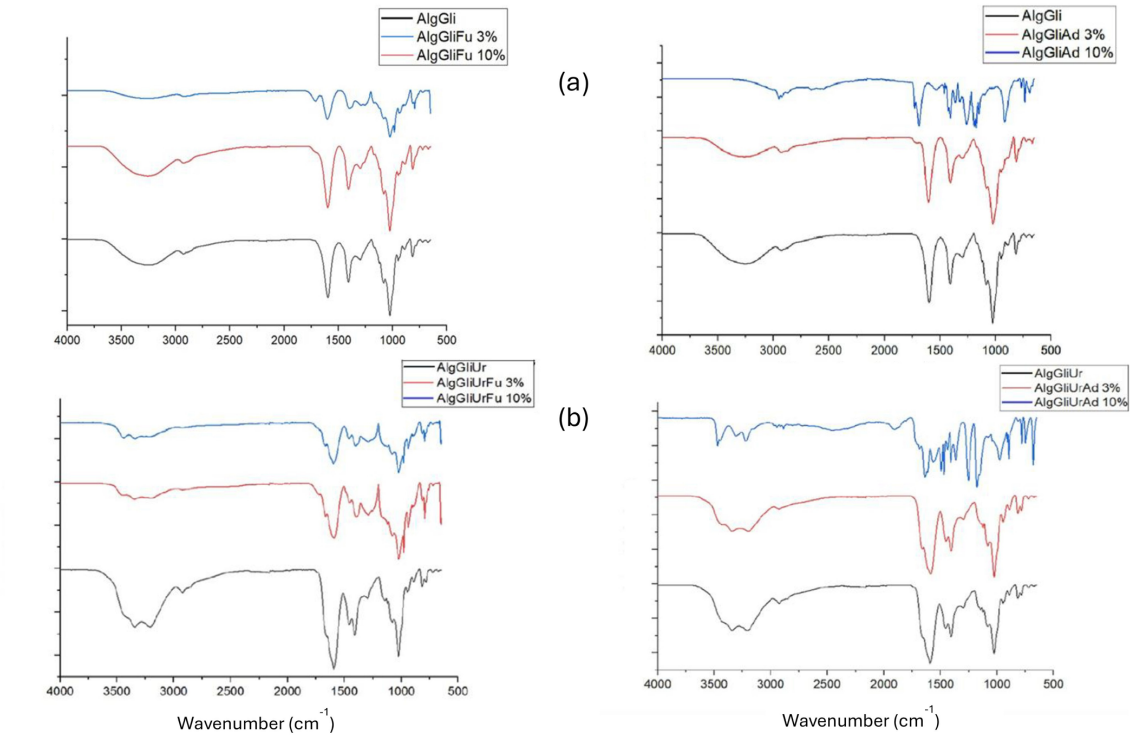

Figure 3. FTIR spectra of films (a) based on alginate (AlgGli), fumaric acid (AlgGliFu), and adipic acid (AlgGliAd), and (b) based on alginate urea (AlgGliUr), fumaric acid (AlgGliUrFu), and adipic acid (AlgGliUrAd) containing 10% glycerol and cross-linked with 3% or 10% (w/w) of acid.

Table 1. Data obtained from TG/DTG curves of urea-modified and unmodified films cross-linked with 3% and 10% w/w of calcium.

Films	Tpeak1 (°C)	Mass loss1 (%)	Tpeak2 (°C)	Mass loss2 (%)	Tpeak3 (°C)	Mass loss3 (%)	Residue (%)
AlgGlCa 3%	53	22	215	30	-	9	39
AlgGlCa 10%	67	15	213	22	263	18	45
AlgGlUrCa 3%	58	19	213	19	255	19	43
AlgGlUrCa 10%	63	18	213	17	258	19	45

At peak1, more precisely between 20 and 150 °C, dehydration of sodium alginate occurred[31]. The mass loss was similar for all samples in this range, with AlgGliCa 3% showing the highest loss and AlgGliCa 10% the lowest. Film degradation starts at 180 °C and in peak2, the degradation of glycerol was observed, and mass loss occurred between 200 and 249 °C[32], with a degradation peak at 213 °C. In peak 2 of AlgGliCa 3%, mass loss was observed at 215 °C. In peak3 of AlgGliCa 10%, cross-linking of calcium with sodium alginate was observed. The residue is similar.

The effects of fumaric acid and adipic acid contents on the thermal degradation profile of the alginate films are shown in Figure 5, and the results are summarized in Table 2.

The 3% and 10% AlgGliAd films present Tpeak1 around 212-215 °C, indicating the occurrence of thermal decomposition reactions of glycerol with a mass loss of approximately 17%. The subsequent mass loss of approximately 37-38% may be associated with the decomposition of the organic components of the film, such as alginate, glycerol, and reaction products of carboxylic acids. Between 220 and 260 °C, degradation of the carboxyl group of sodium alginate occurs with the release of CO_2[33]. After the decomposition of the films, the residues were 45-46%, indicating the presence of nonvolatile materials or reaction products[32].

The AlgGliFu 3% and 10% films also presented peaks (Tpeak1) between 213 °C and 217 °C, indicating thermal

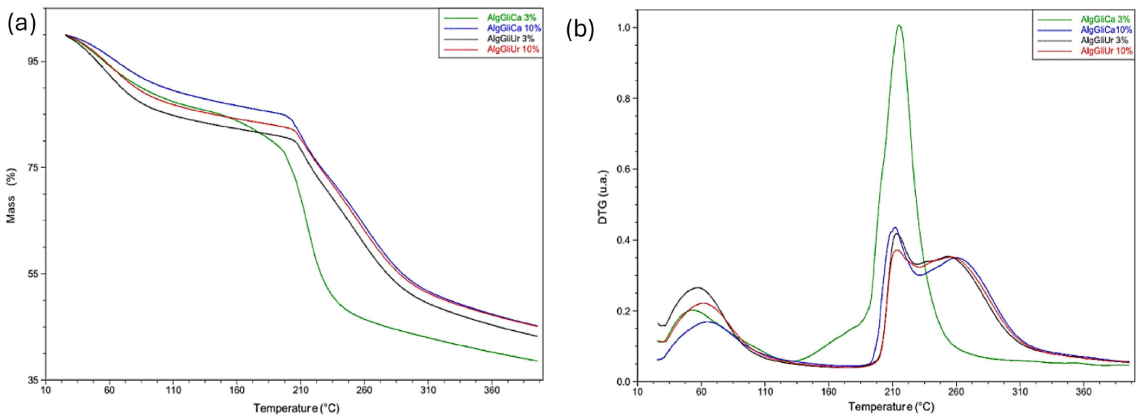

Figure 4. (a) TG and (b) DTG curves of sodium alginate films modified and unmodified with urea and cross-linked with 3% and 10% w/w calcium.

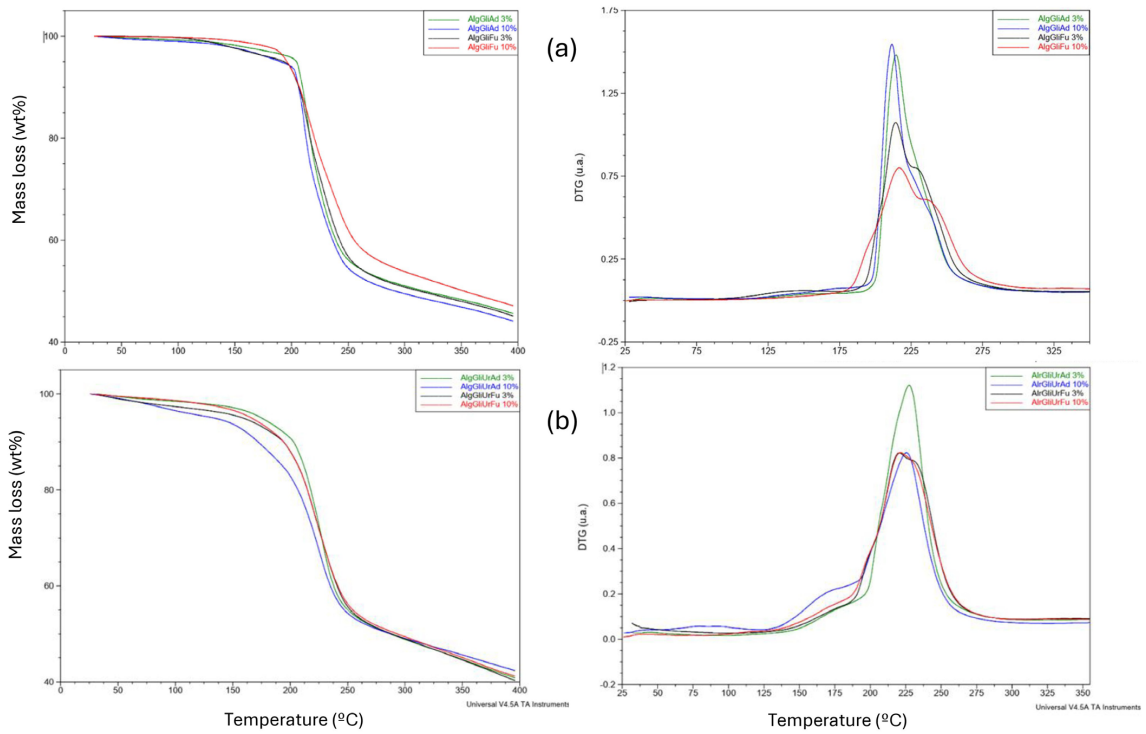

Figure 5. (a) TG and (b) DTG curves of sodium alginate films cross-linked with 3% and 10% w/w fumaric acid or adipic acid.

decomposition reactions of glycerol, although at slightly lower temperatures than those containing adipic acid. A more complex film composition or the occurrence of multiple reactions during decomposition are the reasons for the presence of multiple stages of mass loss. The peaks observed at 225-231 °C may be associated with phase transitions or additional decomposition reactions occurring during the heating of the films, as indicated for films containing alginic acid[26]. The presence of peaks in the formulations with fumaric acid suggests differences in the decomposition kinetics or nature of the reactions compared to the films cross-linked with adipic acid.

The effects of acids on the thermal degradation of urea-containing films demonstrated the presence of two distinct stages of mass loss indicates that the decomposition of the films occurred in stages. The first one is generally associated with the loss of moisture or low-molecular-weight volatiles, whereas the second stage is related to the thermal degradation of the polymeric components. The cross-linker concentrations (3% and 10%) did not appear to significantly affect the temperatures at which mass losses began, indicating that the variation in the amount of adipic acid or fumaric acid did not substantially influence the thermal properties of the films in this specific concentration range.

The absence of peaks at higher temperatures indicates that the thermal decomposition of the films cross-linked with adipic and fumaric acids results in mass loss 2 of approximately 28-29% for adipic acid and 34-35% for fumaric acid. The residue remaining after the decomposition of the films ranged from 40 to 42%. The presence of residues evidences the presence of non-volatile components or reaction products in the sample, and it appeared to be consistent between the different formulations, suggesting that the variation in the adipic acid or fumaric acid concentration did not significantly affect residue formation.

3.3 Differential scanning calorimetry – DSC

The DSC curves of the films of alginate and alginate-urea with glycerol cross-linked with calcium are presented in Figure 6, and the endothermic temperature (Tendo) and exothermic temperature (Texo) data are presented in Table 3.

The curves of the AlgGli and AlgGliUr samples showed broad endothermic peaks at 94 °C and 99 °C, respectively,

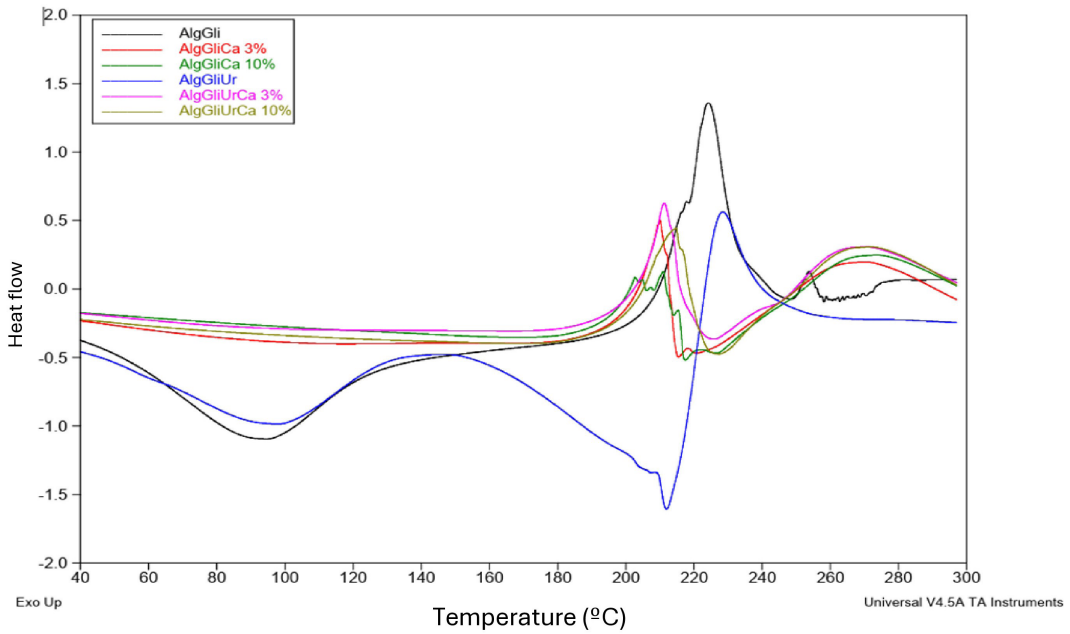

Figure 6. DSC curves of AlgGli samples cross-linked with Ca^{2+} ions.

Table 2. Data from TG/DTG curves of urea-modified and unmodified films cross-linked with 3% and 10% w/w fumaric and adipic acids.

Films	Tpeak1 (°C)	Mass loss1 (%)	Tpeak2 (°C)	Mass loss2 (%)	Residue (%)
AlgGliAd 3%	215	17	-	37	46
AlgGliAd 10%	212	17	-	38	45
AlgGliFu 3%	213	17	225	28	45
AlgGliFu 10%	217	17	231	26	47
AlgGliUrAd 3%	174	31	228	28	41
AlgGliUrAd 10%	170	29	225	29	42
AlgGliUrFu 3%	173	25	220/238	35	40
AlgGliUrFu 10%	174	25	220/238	34	41

attributed to the dehydration process of the films[20]. At the molecular level, the presence of Ca^{2+} ions is considered an obstacle to the rotation (movement) of alginate chains, reducing mobility and, consequently, the ability of the film to elongate[34]. The AlgGliUr sample exhibited a second endothermic event at 212 °C, which can be attributed to the presence of urea[30].

The films cross-linked with calcium (AlgGliCa 3% or 10%) did not exhibit an endothermic peak. However, two exothermic peaks were observed at 210 and 270 °C for the sample with 3% cross-linker and at 211 and 273 °C for the sample with 10%, respectively. The absence of an endothermic peak is explained by the addition of a cross-linker to the film because it causes the union of the chains that are linked by covalent bonds. Therefore, the cross-linked compounds only undergo degradation at high temperatures, so the percentage of cross-linker does not affect the degradation temperatures of the samples[18]. The 3% and 10% AlgGliUrCa films exhibited the same behavior as the AlgGliCa films. The exothermic peaks for these films were 211 and 269 °C with 3% cross-linker and 215 and 271 °C with 10% cross-linker, respectively. It corroborates with FTIR results that part of the urea was removed from the films during the Ca^{2+} crosslinking.

The results for the alginate films cross-linked with adipic acid and fumaric acid are presented in Figure 7 and Table 4.

The Tendo1 of the AlgGliAd 3% film was relatively low, registering 67 °C, and may indicate a phase transition or molecular rearrangement associated with the plasticization of sodium alginate with glycerol[35]. Tendo2 at 178 °C shows

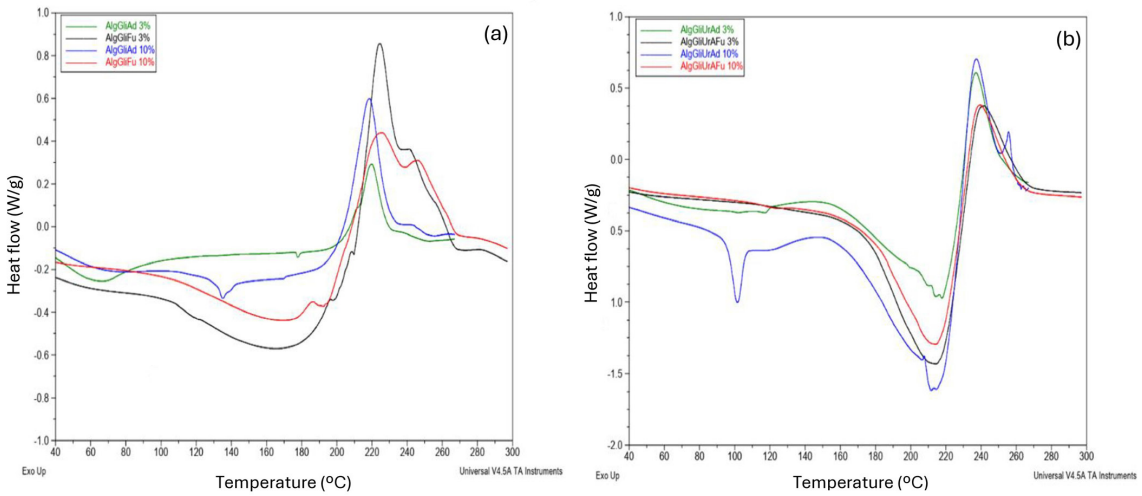

Figure 7. DSC curves of samples (a) AlgGliAd and AlgGliFu and (b) AlgGliUrAd and AlgGliUrFu at 3% and 10% concentration (w/w) of fumaric or adipic acid.

Table 3. Endothermic and exothermic peaks of calcium-cross-linked films.

Films	Tendo1 (°C)	Texo1 (°C)	Texo2 (°C)
AlgGli	94	225	-
AlgGliUr	99/212	229	-
AlgGliCa 3%	-	210	270
AlgGliCa 10%	-	211	273
AlgGliUrCa 3%	-	211	269
AlgGliUrCa 10%	-	215	271

Table 4. Endothermic and exothermic peaks of films with and without urea cross-linked with adipic and fumaric acid.

Films	Tendo1 (°C)	Tendo2 (°C)	Texo1 (°C)	Texo2 (°C)
AlgGliAd 3%	67	178	220	-
AlgGliAd 10%	173	-	224	-
AlgGliFu 3%	135	-	219	-
AlgGliFu 10%	172	192/238	226	247
AlgGliUrAd 3%	118	218	237	-
AlgGliUrAd 10%	215	-	240	-
AlgGliUrFu 3%	101	215/250	238	256
AlgGliUrFu 10%	215	-	240	-

a second thermal transition related to the melting processes or thermal decomposition of components in the film, while Texo1, which was determined to be 220 °C, designates the end of the first thermal transition. For the AlgGliFu 3% film, Tendo1 was 135 °C, a different thermal transition from that observed in AlgGliAd 3%, suggesting variations in the structure or molecular interactions due to fumaric acid as a cross-linker and Texo1 at 220 °C marks the end of the thermal transition. The Tendo1 of the AlgGliAd 10% film was higher than that of AlgGliAd 3%, suggesting a change in the structure of the material due to the increase in the amount of adipic acid as a cross-linker.

The AlgGliUrAd 3%, showed a Tendo1 at 118 °C, and the Tendo2 value was 218 °C, indicating a potential phase transition or crystallization[35] and a second thermal transition that may be related to the melting or thermal decomposition of some components, respectively. While Texo1 was measured at 237 °C, indicating completion of the first thermal transition. The Tendo1 value for AlgGliUrFu 3% was significantly higher than that of AlgGliUrAd 3%, attributed to a different thermal transition, attributed to variations in composition or molecular interactions and, Texo1, measured at 240 °C, can be related to the completion of the thermal transition. Texo1 for AlgGliUrAd 10% films was the lowest among all formulations, registering 101 °C corresponding a change in the structure or composition of the material, possibly owing to an increase in the amount of adipic acid as a cross-linker. Tendo2 showed a wide temperature range, from 215 to 250 °C, and with Texo1 and Texo2 indicate completion of these transitions. The Tendo1 of AlgGliUrFu 10% was similar to that of AlgGliUrAd 10%, meaning that the formulations with 10% cross-linkers shared some thermal properties despite the differences in cross-linkers.

3.4 Dynamic Mechanical Analysis – DMA

The DMA curves of the storage modulus (E') vs. temperature for the alginate and alginate films with fumaric acid or adipic acid permitted estimate the storage modulus and Tan δ values for films at 30 °C (Table 5). For the alginate-urea films urea and those cross-linked with calcium, the results were not possible due to their low tensile strength, indicating more rigid films. It is known that elongation decreased after cross-linking the alginate films with calcium[12]. Once the storage modulus refers to the ability of a material to store energy and deform in phase with the applied stress.

Cross-linking with adipic acid or fumaric acid resulted in a decrease in the stiffness of the films except to the AlgGliFu 3% film that presented the second highest E' value, indicating greater stiffness or elastic energy storage capacity compared to the other films. Adding 3% adipic acid (AlgGliAd 3%) resulted in a 48% decrease in the elastic modulus, while the Tan δ increased, suggesting a greater energy dissipation capacity and a tendency toward more viscoelastic behavior. This decrease in the elastic modulus can be attributed to the formation of additional cross-links between the alginate polymer chains caused by the adipic acid. Conversely, increasing the adipic acid concentration to 10% (AlgGliAd 10%) resulted in an even more pronounced decrease in elastic modulus, accompanied by a slight decline in the Tan δ compared to the 3% formulation. Meaning that more intense cross-linking has a stronger influence on the mechanical properties of the film, although the energy dissipation capacity remained relatively stable.

The AlgGliFu 3% formulation presented an elastic modulus comparable to AlgGli but with a slightly lower Tan δ, indicating a lower energy dissipation capacity. However, the AlgGliFu 10% formulation showed a significant reduction in the elastic modulus, accompanied by a considerable increase in Tan δ, suggesting a transition to more viscoelastic behavior and a greater energy dissipation capacity. This can be attributed to the formation of additional cross-links induced by fumaric acid, which has a more pronounced impact on the mechanical properties of the film. These films exhibit an elastic response, deformation, and an increase in their storage modulus with increasing temperature.

When analyzing a typical DMA result, it was observed a rapid decline in E' and a peak in the Tan δ curve[36]. This transition is called the α transition or glass transition (Tg). This temperature is associated with significant variations in the material properties[37].

3.5 Biodegradation test

The films were prepared with alginate and alginate-urea were divided by the cross-linking process and are shown in Figure 8.

During the tests, the film fragments adhered to the casings, and there was a significant accumulation of soil. The alginate films cross-linked with acids showed fragments remaining in the casing, whereas the modified alginate films were more resistant, presenting less fragmentation. After 21 days, alginate films modified with urea and cross-linked with different acids began a greater fragmentation process than films based solely on alginate. After 42 days of burial in the soil, all alginate and modified alginate films showed a significant reduction in size and yellowing (see yellow rectangle in Figure 8).

In the modified alginate films cross-linked with calcium ions, the samples became thinner and more brittle. Regarding the films cross-linked with Ca^{2+} ions, a similar behavior was observed for the films cross-linked with acid, that is, shrinkage and yellowing, and all of them, although deformed, remained partially structured over the 42 days of the study. The literature reports that biofilms explored for packaging, based on xylan and xylan/gelatin plasticized with glycerol showed biodegradability in soil for 30 days[38].

Table 5. Storage modulus and Tan δ values for films at 30 °C.

Films	E' (MPa)	Tan δ	Films	E' (MPa)	Tan δ
AlgGli	2378	0.09			
AlgGliAd 3%	1142	0.31	AlgGliFu 3%	2600	0.11
AlgGliAd 10%	630	0.28	AlgGliFu 10%	370	0.33

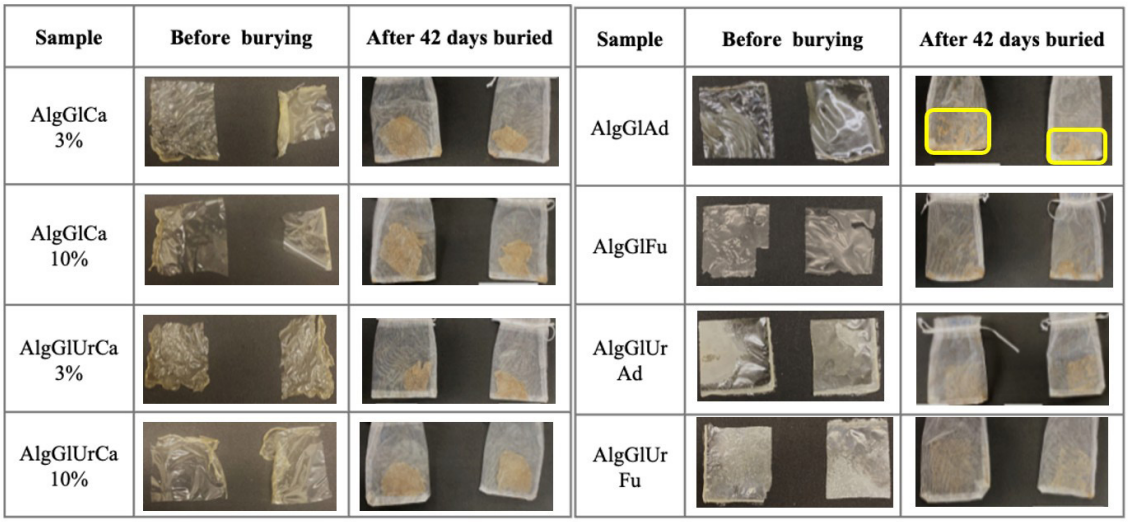

Figure 8. Biodegradation test images of the films in the soil before and after 42 days.

While a certain degree of biodegradability for films based on chitosan plasticized with glycerol was observed over 17 weeks[32]. Films made from *Solanum lycocarpum* St. Hill starch plasticized with glycerol (5-20%) were completely degraded over 180 days[39]. This preliminary assessment of the behavior of alginate films modified with urea and cross-linked with different acids and Ca^{2+} ions demonstrated a degradation profile between that of other biodegradable films used for packaging.

4. Conclusions

TGA and DSC analyses revealed that the modified and cross-linked films exhibited an excellent resistance to thermal degradation, indicating superior stability under high-temperature conditions. In addition, FTIR analyses provided information on the molecular interactions in the films, indicating the formation of cross-links between the functional groups of sodium alginate, glycerol, and cross-linking agents. The results indicated that the modification of alginate films with glycerol and cross-linking with adipic acid or fumaric acid significantly affected their mechanical and viscoelastic properties.

The following conclusions were drawn regarding the biodegradation of alginate and modified alginate films in soil using different cross-linkers. Visual analyses were essential for assessing the morphology of the films, highlighting changes in their appearance and structural integrity over time. Variations in the concentrations of additives led to different biodegradation rates, which suggests the feasibility of tailoring the biodegradation of the films to meet specific application requirements, thus enhancing their potential use in structures that are intended for burial in soil.

5. Author's Contribution

- **Conceptualization** – Nivaldo Ramos Júnior; Ana Paula Testa Pezzin; Denise Abatti Kasper Silva
- **Data curation** – Nivaldo Ramos Júnior; Denise Abatti Kasper Silva
- **Formal analysis** – Nivaldo Ramos Júnior; Ana Paula Testa Pezzin; Denise Abatti Kasper Silva
- **Funding acquisition -** Ana Paula Testa Pezzin; Denise Abatti Kasper Silva
- **Investigation** – Nivaldo Ramos Júnior; Denise Abatti Kasper Silva
- **Methodology** – Nivaldo Ramos Júnior; Ana Paula Testa Pezzin; Denise Abatti Kasper Silva
- **Project administration** – Ana Paula Testa Pezzin; Denise Abatti Kasper Silva
- **Resources** – Nivaldo Ramos Júnior; Denise Abatti Kasper Silva
- **Software** – NA.
- **Supervision** – Nivaldo Ramos Júnior; Ana Paula Testa Pezzin; Denise Abatti Kasper Silva
- **Validation** – Nivaldo Ramos Júnior; Ana Paula Testa Pezzin; Denise Abatti Kasper Silva
- **Visualization** – Nivaldo Ramos Júnior; Ana Paula Testa Pezzin; Denise Abatti Kasper Silva
- **Writing – original draft** – Nivaldo Ramos Júnior; Ana Paula Testa Pezzin; Denise Abatti Kasper Silva
- **Writing – review & editing** – Ana Paula Testa Pezzin; Denise Abatti Kasper Silva

6. Acknowledgments

This research work was funded by the Brazilian Coordination for the Improvement of Higher Education Personnel (CAPES).

7. References

1. Food and Agriculture Organization of the United Nations – FAO. (2021). *Assessment of agricultural plastics and their sustainability: a call for action.* Rome: FAO. https://doi.org/10.4060/cb7856en.

2. Wawszczak, A., Kocki, J., & Kołodyńska, D. (2024). Alginate as a sustainable and biodegradable material for medical and environmental applications: the case studies. *Journal of Biomedical Materials Research. Part B, Applied Biomaterials*, *112*(9), e35475. https://doi.org/10.1002/jbm.b.35475. PMid:39269132.
3. Rahman, M. M., Shahid, M. A., Hossain, M. T., Sheikh, M. S., Rahman, M. S., Uddin, N., Rahim, A., Khan, R. A., & Hossain, I. (2024). Sources, extractions, and applications of alginate: a review. *Discover Applied Sciences*, *6*(8), 443. https://doi.org/10.1007/s42452-024-06151-2.
4. Qamar, S. A., Qamar, M., Basharat, A., Bilal, M., Cheng, H., & Iqbal, H. M. N. (2022). Alginate-based nano-adsorbent materials: bioinspired solution to mitigate hazardous environmental pollutants. *Chemosphere*, *288*(Pt 3), 132618. https://doi.org/10.1016/j.chemosphere.2021.132618. PMid:34678347.
5. Benettayeb, A., Guibal, E., Morsli, A., & Kessas, R. (2017). Chemical modification of alginate for enhanced sorption of Cd(II), Cu(II) and Pb(II). *Chemical Engineering Journal*, *316*, 704-714. https://doi.org/10.1016/j.cej.2017.01.131.
6. Llive, L. M., Perullini, M., Santagapita, P. R., Schneider-Teixeira, A., & Deladino, L. (2020). Controlled release of fertilizers from Ca(II)-alginate matrix modified by yerba mate (*Ilex paraguariensis*) waste. *European Polymer Journal*, *138*, 109955. https://doi.org/10.1016/j.eurpolymj.2020.109955.
7. Lüdke, J. V. (1993). *Efeito da inclusão de ácido fumárico em rações com dois níveis de derivados lácteos sobre o desempenho de leitões desmamados aos 23 dias de idade* (Master's dissertation). Universidade Federal do Rio Grande do Sul, Porto Alegre.
8. Fujimoto, M. C. M. (2018). *Modelagem e simulação de biorreator para produção de ácido fumárico* (Undergraduate thesis). Universidade Federal de São Carlos, São Carlos. Retrieved in 2025, August 30, from https://repositorio.ufscar.br/handle/20.500.14289/15023
9. Ilica, R.-A., Kloetzer, L., Galaction, A.-I., & Caşcaval, D. (2019). Fumaric acid: production and separation. *Biotechnology Letters*, *41*(1), 47-57. https://doi.org/10.1007/s10529-018-2628-y. PMid:30506453.
10. Sivashankari, P. R., & Prabaharan, M. (2017) *Deacetylation modification techniques of chitin and chitosan.* In J. A. Jennings, & J. D. Bumgardner (Eds.), *Chitosan based biomaterials* (pp. 117-133). Amsterdam: Woodhead Publishing. https://doi.org/10.1016/B978-0-08-100230-8.00005-4.
11. van der Merwe, R. T., Goosen, N. J., & Pott, R. W. M. (2022). Macroalgal-derived alginate soil amendments for water retention, nutrient release rate reduction, and soil pH control. *Gels*, *8*(9), 548. https://doi.org/10.3390/gels8090548. PMid:36135260.
12. Tan, J., Luo, Y., Guo, Y., Zhou, Y., Liao, X., Li, D., Lai, X., & Liu, Y. (2023). Development of alginate-based hydrogels: crosslinking strategies and biomedical applications. *International Journal of Biological Macromolecules*, *239*, 124275. https://doi.org/10.1016/j.ijbiomac.2023.124275. PMid:37011751.
13. Maity, C., & Das, N. (2021). Alginate-based smart materials and their application: recent advances and perspectives. *Topics in Current Chemistry (Cham)*, *380*(1), 3. https://doi.org/10.1007/s41061-021-00360-8. PMid:34812965.
14. Gebresas, G. A., Szabó, T., & Kálmán Marossy, K. (2023). A comparative study of carboxylic acids on the cross-linking potential of corn starch films. *Journal of Molecular Structure*, *1277*, 134886. https://doi.org/10.1016/j.molstruc.2022.134886.
15. Coma, V., Sebti, I., Pardon, P., Pichavant, F. H., & Deschamps, A. (2003). Film properties from crosslinking of cellulosic derivatives with a polyfunctional carboxylic acid. *Carbohydrate Polymers*, *51*(3), 265-271. https://doi.org/10.1016/S0144-8617(02)00191-1.
16. Brioude, M. M., Guimarães, D. H., Fiúza, R. P., Prado, L. A. S. A., Boaventura, J. S., & José, M. N. (2007). Synthesis and characterization of aliphatic polyesters from glycerol, by-product of biodiesel production, and adipic acid. *Materials Research*, *10*(4), 335-339. https://doi.org/10.1590/S1516-14392007000400003.
17. Sigma-Aldrich. (2023). *Ficha de dados de segurança: ácido adípico.* Retrieved in 2025, August 30, from https://www.sigmaaldrich.com/BR/pt/sds/sigma/a26357?userType=anonymous
18. Yang, S. T., Zhang, K., Zhang, B., & Huang, H. (2011). *Fumaric acid.* In: M. Moo-Young (Ed), *Comprehensive biotechnology* (pp. 163-177). Oxford: Pergamon. https://doi.org/10.1016/B978-0-08-088504-9.00456-6.
19. Wodtke, M. E. F., Apati, G. P., & Silva, D. A. K. (2023). Produção e caracterização de filmes à base de alginato visando à aplicação na área ambiental. *Caderno de Iniciação à Pesquisa*, *25*, 168-174. Retrieved in 2025, August 30, from https://www.univille.edu.br/account/pesquisa/VirtualDisk.html/downloadDirect/3539631/Caderno_de_Iniciacao_a_Pesquisa_Cientifica_PIBIC_2023_-_Volume_25.pdf
20. Leal, D., Matsuhiro, B., Rossi, M., & Caruso, F. (2008). FT-IR spectra of alginic acid block fractions in three species of brown seaweeds. *Carbohydrate Research*, *343*(2), 308-316. https://doi.org/10.1016/j.carres.2007.10.016. PMid:18048014.
21. Custódio, A. C., Ribeiro, R. P. S., Lima, T. B. S. L., Araújo, E. S., & Araújo, P. L. B. (2022). Purificação simplificada do rejeito de glicerina bruta da produção de biodiesel da biorrefinaria Berso-UFPE: uma prática sustentável. *Revista Brasileira de Geografia Física*, *15*(5), 2226-2237. https://doi.org/10.26848/rbgf.v15.5.p2226-2237.
22. Draget, K. I., Smidsrød, O., & Skjåk-Bræk, G. (2005). *Alginates from algae.* In A. Steinbüchel (Ed.), *Biopolymers online.* Weinheim: Wiley-VCH. https://doi.org/10.1002/3527600035.bpol6008.
23. Manivannan, M., & Rajendran, S. (2011). Investigation of inhibitive action of urea-Zn^{2+} system in the corrosion control of carbon steel in sea water. *International Journal of Engineering Science and Technology*, *3*(11), 8048-8060. Retrieved in 2025, August 30, from https://www.researchgate.net/publication/267782937_Investigation_of_inhibitive_action_of_urea-Zn2_system_in_the_corrosion_control_of_carbon_steel_in_sea_water
24. Piasek, Z., & Urbanski, T. (1962). The infrared absorption spectrum and the structure of urea. *Bulletin de l'Académie Polonaise des Sciences. Série des Sciences Chimiques*, *10*, 113-120.
25. Fransiska, D., Abdullah, A. H. D., Nurhayati, Irianto, H. E., Nissa, R. C., Sedayu, B. B., Syamani, F. A., Raharjo, S., Suwarti, & Agusman, (2024). Impact of agar–glycerol ratios on the physicochemical properties of biodegradable seaweed films: A compositional study. *International Journal of Biological Macromolecules*, *280*(Pt 3), 135855. https://doi.org/10.1016/j.ijbiomac.2024.135855. PMid:39317277.
26. Fan, Y., Xu, J., Gao, X., Fu, X., & Yang, X. (2019). Effect of alginate on the release of amide nitrogen for soilless cultivation applications. *Scientia Horticulturae*, *256*, 108545. https://doi.org/10.1016/j.scienta.2019.108545.
27. Escobar-Avello, D., Ferrer, V., Bravo-Arrepol, G., Reyes-Contreras, P., Elissetche, J. P., Santos, J., Fuentealba, C., & Cabrera-Barjas, G. (2023). Pretreated *Eucalyptus globulus* and *Pinus radiata* barks: potential substrates to improve seed germination for a sustainable horticulture. *Forests*, *14*(5), 991. https://doi.org/10.3390/f14050991.
28. Marangoni, L., Jr., Rodrigues, P. R., Silva, R. G., Vieira, R. P., & Alves, R. M. V. (2021). Sustainable packaging films composed of sodium alginate and hydrolyzed collagen: preparation and characterization. *Food and Bioprocess Technology*, *14*(12), 2336-2346. https://doi.org/10.1007/s11947-021-02727-7.

29. Larosa, C., Salerno, M., Lima, J. S., Meri, R. M., Silva, M. F., Carvalho, L. B., & Converti, A. (2018). Characterisation of bare and tannase-loaded calcium alginate beads by microscopic, thermogravimetric, FTIR and XRD analyses. *International Journal of Biological Macromolecules*, *115*, 900-906. https://doi.org/10.1016/j.ijbiomac.2018.04.138. PMid:29704606.
30. Pratinthong, K., Punyodom, W., Jantrawut, P., Jantanasakulwong, K., Tongdeesoontorn, W., Sriyai, M., Panyathip, R., Thanakkasaranee, S., Worajittiphon, P., Tanadchangsaeng, N., & Rachtanapun, P. (2024). Modification of a carboxymethyl cellulose/poly(vinyl alcohol) hydrogel film with citric acid and glutaraldehyde crosslink agents to enhance the anti-inflammatory effectiveness of triamcinolone acetonide in wound healing. *Polymers*, *16*(13), 1798. https://doi.org/10.3390/polym16131798. PMid:39000654.
31. Hou, L., & Wu, P. (2019). Exploring the hydrogen-bond structures in sodium alginate through two-dimensional correlation infrared spectroscopy. *Carbohydrate Polymers*, *205*, 420-426. https://doi.org/10.1016/j.carbpol.2018.10.091. PMid:30446124.
32. Santana, M. C. C. B. (2012). *Formulação, caracterização e eficácia antioxidante de filmes biodegradáveis ativos a base de quitosana, glicerol e aditivos naturais* (Master's dissertation). Universidade Federal da Bahia, Salvador.
33. Wang, B., Wan, Y., Zheng, Y., Lee, X., Liu, T., Yu, Z., Huang, J., Ok, Y. S., Chen, J., & Gao, B. (2018). Alginate-based composites for environmental applications: a critical review. *Critical Reviews in Environmental Science and Technology*, *49*(4), 318-356. https://doi.org/10.1080/10643389.2018.1547621. PMid:34121831.
34. Turbiani, F. R. B., Kieckbusch, T. G., & Gimenes, M. L. (2011). Release of calcium benzoate from films of sodium alginate cross-linked with calcium ions. *Polímeros Ciência e Tecnologia*, *21*(3), 175-181. https://doi.org/10.1590/S0104-14282011005000034.
35. Cacuro, T. A. (2019). *Compósitos de alginato como material inteligente, modulação de solubilidade e objeto de ensino* (Doctoral thesis). Universidade Federal de São Carlos, São Carlos. Retrieved in 2025, August 30, from https://repositorio.ufscar.br/handle/20.500.14289/12093
36. Lorandi, N. P. A., Cioffi, M. O. H., & Ornaghi, H., Jr. (2016). Dynamic Mechanical Analysis (DMA) of polymeric composite materials. *Scientia Cum Industria*, *4*(1), 48-60. https://doi.org/10.18226/23185279.v4iss1p48.
37. Moura, M. F. S., Morais, A. B., & Magalhães, A. G. (2005). *Materiais compósitos: materiais, fabrico e comportamento mecânico*. Porto: Publindústria.
38. Lucena, C. A. A., Costa, S. C., Eleamen, G. R. A., Mendonça, E. A. M., & Oliveira, E. E. (2017). Desenvolvimento de biofilmes à base de xilana e xilana/gelatina para produção de embalagens biodegradáveis. *Polímeros*, *27*(spe), 35-41. https://doi.org/10.1590/0104-1428.2223.
39. Fernandes, A. S., Cardoso, J. C. O., Gomes, J. N., & Ascheri, D. P. R. (2019). Elaboração e caracterização de filmes biodegradáveis de amido de *Solanum lycocarpum* St. Hill e glicerol. *Fronteira: Journal of Social, Technological and Environmental Science*, *8*(1), 362-378. https://doi.org/10.21664/2238-8869.2019v8i1.p362-378.

Received: Aug. 30, 2025
Revised: Nov. 26, 2025
Accepted: Dec. 03, 2025

Editor-in-Chief: *Sebastião V. Canevarolo*